Torsional Effects on Wind Turbine Blades and Impact on Field Damages

F. M. Jensen[1], J. O. Arconada[1], M. Werk[1], C. Berggreen[2], J. D. Sørensen[3], G. Zhong[4], W. Haans[4]

[1]Bladena, Banestrøget 13, 2630 Taastrup, Denmark.

[2]Technical University of Denmark, Department of Civil and Mechanical Engineering, Koppels Allé, Building 404, 2800 Kgs. Lyngby, Denmark.

[3]AAU, Department of The Built Environment, Thomas Manns Vej 23, 9220 Aalborg, Denmark.

[4]Shell Global Solutions International B.V., 2596 HR Den Haag, Netherlands.

17th of July

Email: fmj@bladena.com

Abstract.
The purpose of this paper is to present the importance of torsional loads when understanding the significant increase in structural damages on large wind turbine blades. By comparing the stress state of two blades of different length, it is shown that torsional loads grow with an exponent of four (4). Thereby, a function of the length of the blades leading to a new range of challenges that are not met by the current process for design, testing and certification.

The paper presents the study of these new challenges in detail, based upon:
- An experimental perspective, with results from large-scale cyclic loading tests on two blade cut-outs conducted under controlled laboratory conditions in. Both blades were tested to failure.
- A numerical perspective, non-linear geometrical 3D FEM simulations has been performed to study the impact of torsional loads on relevant current structural failure modes on large wind turbine blades.

The conclusion is that the larger torsional loads may explain shear-web disbond, as well as sandwich skin debonding in both the transition zone and in the max chord area of wind turbine blades. In view of the findings, the paper includes proposals for remedies that are expected to mitigate some of the significant failures currently seen in the field.

1. Abbreviations

Leading edge	LE
Trailing edge	TE
Pressure side	PS
Suction side	SS
Cross-Sectional Shear Distortion	CSSD
Root torsional moment	RTM
Root bending moment	RBM
Number of cycles to failure for given cyclic stress of specific material	S-N curves
Trailing edge Towards Leading edge	TTL

Table 1. *List of abbreviations*

2. Introduction

2.1. Background

Publications in recent years have highlighted an increase in structural blade failures (ref.[2.], [5.], [11.]), a fact that has been recognized not only by wind turbine owners, but also by manufacturers and certification bodies (ref.[2.]).

Published articles, see ref. [1.-14.], report reoccurring blade issues on several platforms with large blades on 5MW to 8MW turbines. In some of the reported blade collapses, the operators have shown concern that the critical damage is not a one-off event (ref.[5.]).. Therefore studies have been conducted of whole fleets such as in 2021 at a Norwegian wind farm, see ref.[2] and in 2020 at a wind farm in the USA, see ref.[3]. Furthermore, DNV has recently published a whitepaper acknowledging the relevance of the topic, see ref.[2].

The trend that structural related failures occur early at the large blade's lifetime, suggests that the methodologies used in the development and testing phase of blades need improvements, see ref.[4]. In some instances when similar blade failure happens on the same platform on different wind farms, it can be a clear sign of insufficient testing of the specific blade type, see ref.[5].

The importance of torsional loading is becoming an increasingly significant topic, as found in the studies performed for different blade sizes and presented in this paper. These studies have clearly demonstrated that increasing the length of the blades only adds to the severity of the challenges.

A comprehensive analysis of the importance of the torsional loads for large blades is presented in this paper. According to the current testing standards (ref.[19.]), both edgewise and flapwise load cases are required, but not the operational load case. For large blades, edgewise loading is often the most critical and is therefore used for comparison in this paper. However, neither the edgewise nor the flapwise test load cases include significant torsional loads.

The reason why this topic has been addressed is the rising concerns that out-of-plane panel deformations is a major root cause of critical stresses in adhesive bondlines as well as between the composite layers (interlaminar stresses), especially, the interface between sandwich skin and sandwich core materials. The term sandwich skin is used in this context to refer to the face sheets, thus the outer- or inner-most layers of sandwich panels.

2.2. Torsional Loads Overview

The current design basis considers the loads associated with displacements in the edgewise and flapwise independently and not their combined three-dimensional effect equivalent to what is found under actual operating conditions.

Figure 1 shows the three-dimensional tip deflection in both directions when the blade is in operation. This deflection is a consequence of the combination of flapwise loads due to the aerodynamic impact of

the incoming wind, and edgewise loads, due to gravity forces and blade dynamics during rotation. These movements cause forces to act not exactly at the blade's shear centre, thereby creating an arm that generates a Root Torsional Moment (RTM). The direction of this RTM depends on the magnitude of the applied loads and the stiffness of the blade. The load contributions that introduce a root torsional moment on the blade arise from the aerodynamic forces and gravity working on the already deformed blade under operation. As blades increase in length, the tip deflection also increases significantly, leading to notable rise in the RTM. This will be further discussed in the subsequent section of the paper.

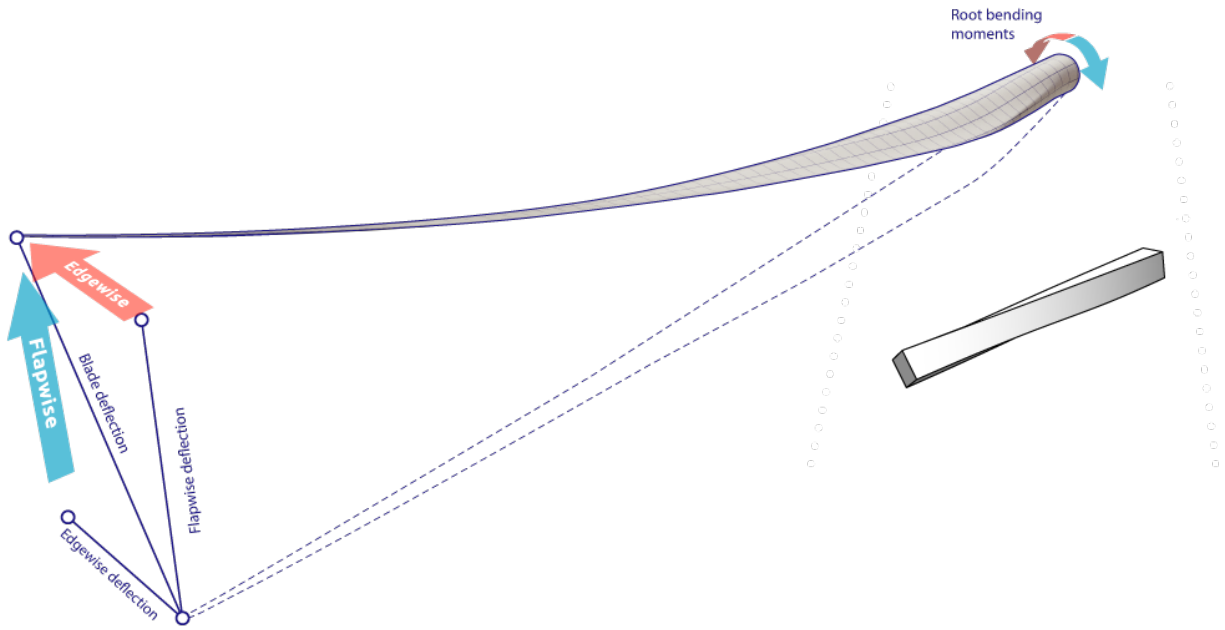

Figure 1. Flapwise and edgewise load components and tip deflection generate Root Torsional Moments (RTM). The orange arrow at the tip represents the edgewise aerodynamic tangential forces and the corresponding root bending moment at the root. The blue arrow at the tip represents the flapwise aerodynamic tangential forces and the corresponding root bending moment at the root. The arrows are representive, the forces act along the whole blade.

Seen from tip towards the root, the edgewise aerodynamic loads working on a flapwise deformed blade twist the blade in a clockwise direction and the flapwise loads generate a counterclockwise twist to the blade. The torsional load components cause localized panel deformations in the transition zone and in the max chord area of the blade (ref.[13.]). As a result of out-of-plane deformation, bending strains in the panels are generated. This occurs mainly in the transition zone and in the max chord area. The deformations also cause peeling stresses in the bondlines of blade designs with an aft shear web.

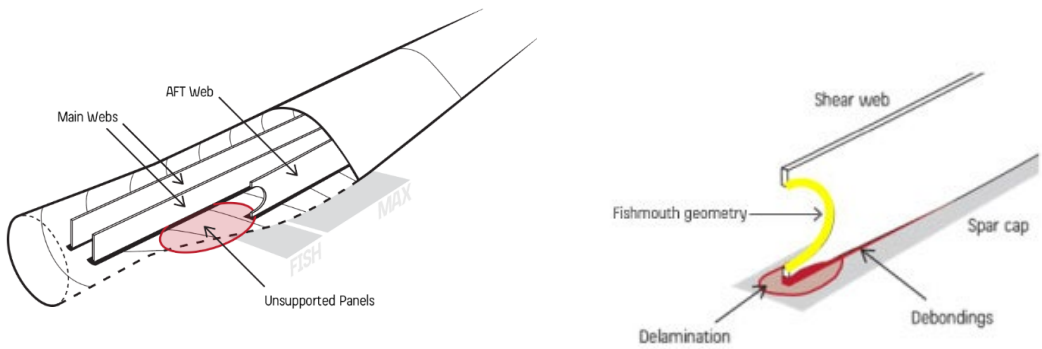

Figure 2. Transition zone of blade with 2 main shear webs and one aft shear web with unsupported panels, the red ellipse illustrating the area where the unsupported panels are located (left). Connection between the aft shear web fishmouth and the spar cap. Highlighted, initiation of delamination and debonding (right).

Localized bending of the sandwich panels in the transition zone (see Figure 3 for further information about the transition zone), often results in peeling in the bondlines of blade designs with an aft shear web. This occurs more frequently due to the peeling stresses caused by the out-of-plane deformation of the unsupported panels, which are carried by the bondlines of the aft shear web. In blades without an aft shear web, the peeling stresses are carried by the bondlines in the trailing edge and at the main shear web.

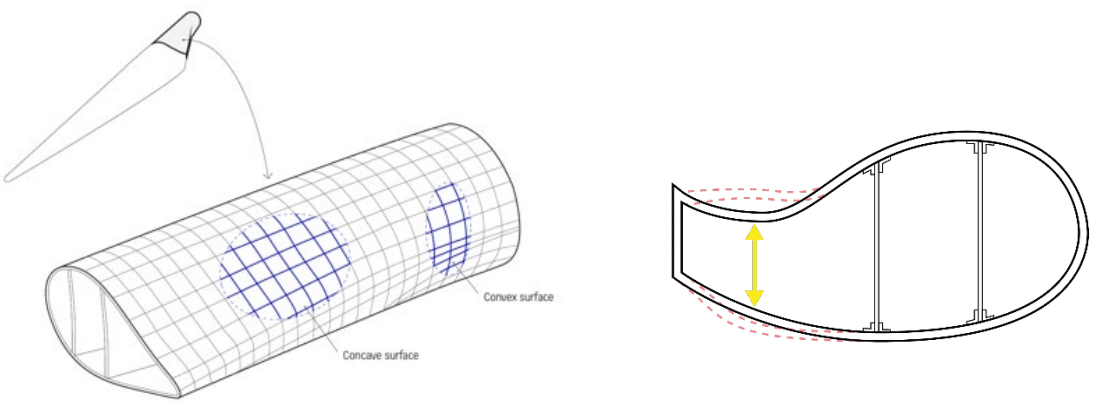

Figure 3. Transition zone of a large blade where the complex geometry can be appreciated, moving from a convex to concave shape, and changing in tapering in 3 directions. On the right, localized bending of the panels is represented, the solid lines represent the un-deformed positions, and the dashed lines present the deformed positions.

Furthermore, the torsional loads cause additional cross-sectional shear distortion (CSSD), which results in additional peeling stresses (ref. [13.]) being transferred to the bondlines, see Figure 4. This phenomenon is in many cases driving structural related failures early in the lifetime of large wind turbine blades, see ref. [1]. In a previous study conducted by Bladena, it was concluded that both cross sectional shear distortion, and especially out-of-plane deformation of the panels in the transition zone, are the two main root causes of shear-web disbonding in the transition zone, see ref.[9].

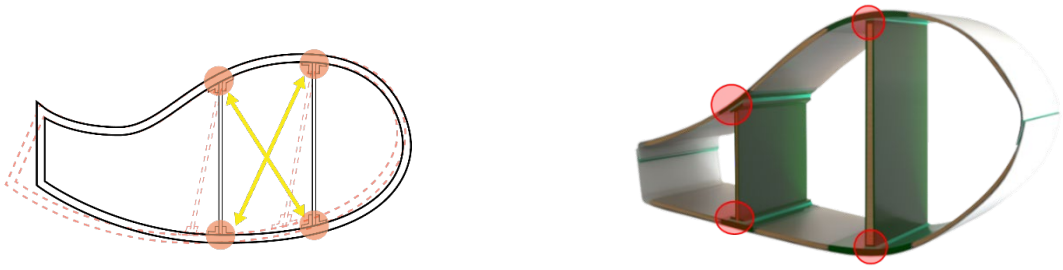

Figure 4. Blade cross-section. On the left, the solid lines represent the un-deformed position wand the dashed lines show the deformed position. On the right, bondlines highlighted in red circles on a blade cross section.

The significance of the torsional loads and the associated deformations is tied to the fact that they increase with a power of 4 in relation with the length of the blades. This will be presented in the paper in more details in section 4. Hence, what was considered an acceptable risk for a certain size of blade may become out of control as the blades increase in length, even leading to failures shortly after the blades have entered into operation.

The paper presents results of non-linear geometric 3D-solid FEM simulations to quantify these phenomena.

3. Experimental analysis: Large-scale testing applying torsional fatigue loads

3.1. Background and experimental methods

A large-scale test campaign was performed by utilizing the strong-floor test facilities. The purpose of the test campaign was to demonstrate the impact of torsional loads on a blade's transition zone region. A detailed description of the test program is presented in ref.[6]. Based on the 3D FEM analysis - as a direct impact of torsional loading - significant out-of-plane panel deformation occurs in the blade sandwich shells on both pressure and suction side. This oscillatory out-of-plane panel deformation is generating peeling stresses in the adhesive bondline connecting the aft shear web to the shells.

The blade type used for this test campaign was a 34m blade manufactured by SSP Technology using a prepreg manufacturing process (pre-impregnated fiber mats without autoclave) (ref. [17.]). High resin content was selected for the laminates close to the PVC foam core and mold to ensure adequate resin quantity According to the manufacturer a modification of the Ampreg 22 epoxy laminating system was used (ref. [18.]). Although, this blade type is considerably smaller than the blades typically discussed when addressing failure in the transition zone and newer blade designs are more likely to use balsa wood or PET foam for the core material. Despite, it is still sufficient to develop the test method and to demonstrate the effect of torsional loads with the use of right setup. A 15m root end section cut-out of the SSP34m blade was utilized with a retrofitted aft shear web in the transition zone. Since the blade originally has a box spar design, a retrofit aft shear web was necessary (ref. [15]). This web was installed 4m from the root towards the tip section, positioned midway between the load carrying box girder and the trailing edge. The position was determined based on previously conducted test results which indicated the highest out-of-plane deformation in this area, see ref. [1.]). The main body of the aft shear web is a sandwich structure consisting of a 10mm core material (PVC foam) and four layers of bi-axial glass fiber. The strong-floor setup and the retrofitted aft shear web are presented on the Figure 5.

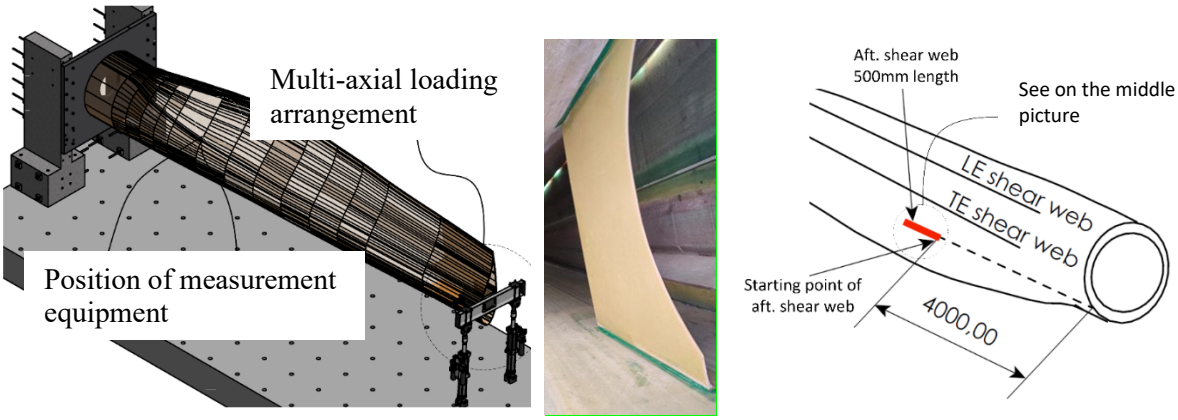

Figure 5. Large-scale strong-floor based test setup, the root section is mounted on a vertical strong-floor and the tip end is mounted onto the load train, the load introduction is explained on Figure 6 (left). Retrofitted aft shear installed in the 2 blade cut-outs (middle). The position of the retrofitted aft shear web illustrated (right).

Since the large-scale test was performed on the inner 15m section containing the transition zone, it is noted that the large-scale test will not be able to address one of the main conclusions explained below in subsection 4.2. Here the deflection of the tip of a large blade gets significantly amplified when both edgewise and flapwise loads are acting simultaneously, creating a large torsional arm that will lead to a high torsion on the structural regions of the blade.

In order to account for this limitation, and to avoid a testing campaign that could last for multiple years using conventional full-scale blade test methodologies, an accelerated fatigue test was carried out using the large-scale test setup and section test configuration. Thus, the loads applied are higher than the tested blade would ever experience in field conditions. Also, the layout and geometrical characteristics of the tested blade differs from current large blade types. Nonetheless, results from the test are illustrative of the field scenario for larger blades.

The torsional cyclic loads which have been applied in the large-scale tests are 50% higher than those that a 1.5MW old blade will meet in the field. The reason is that the objective is to demonstrate the importance of torsional loads on a larger blade. Ideally, a large modern blade should have been tested, but that has not been possible within the framework and budget of this research project.

The loading arrangement consists of two structural actuators which are capable of applying loads at the free end of the root section compromising two degree-of-freedoms: edgewise load along with torsional moment around the longitudinal axis of the blade. The maximum loading used during this fatigue test was 100kN edgewise load component (F_Y) and 100kNm as torsional moment (M_Z) respectively and with a frequency of 0.1Hz. Figure 6 below shows the test setup actuator configuration of the loading at the 15m reinforced cross-section. More details about the test setup can be found in ref. [7]. Figure 6 illustrates the test setup and the actuator specifications with the related coordinate system. During the test campaign various instruments were used, including a Digital Image Correlation (DIC) system, 4 strain gauges mounted on the retrofitted aft shear web, acoustic emission sensors and a wire potentiometer, more details about the instrumentation (e.g., instrument specification, positioning, etc.) see in ref. [7.]. The illustration shows the mounted position of the blade on the test rig and visualizes the applied load components.

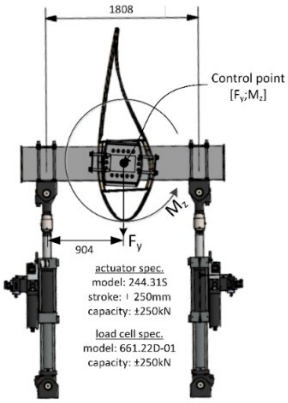

Figure 6. Active coordinate system and notation of the load train. Source: ref. [7]

3.2. Experimental results

The test resulted in a critical damage in the transition zone area on the pressure side panel in the trailing edge region of the blade in approx. 280.000 load cycles. More info about the damage and the test can be found in ref. [7.]. Further testing on the same blade section would have led to a blade collapse due to significant sudden decrease in edgewise stiffness (see Figure 7). This damage was a direct result of the applied torsional fatigue loads, causing large-scale damage on the blade shell in the root transition zone due to delamination from the out-of-plane deformation. The damage is shown on Figure 7. Such damage is considered critical, as it would require an immediate action if it happened during operation; failure to do so could potentially lead to further structural damage to the blade or other areas of the wind turbine. as if no actions were taken it could potentially lead to further structural damages on the blade or on other areas of the wind turbine.

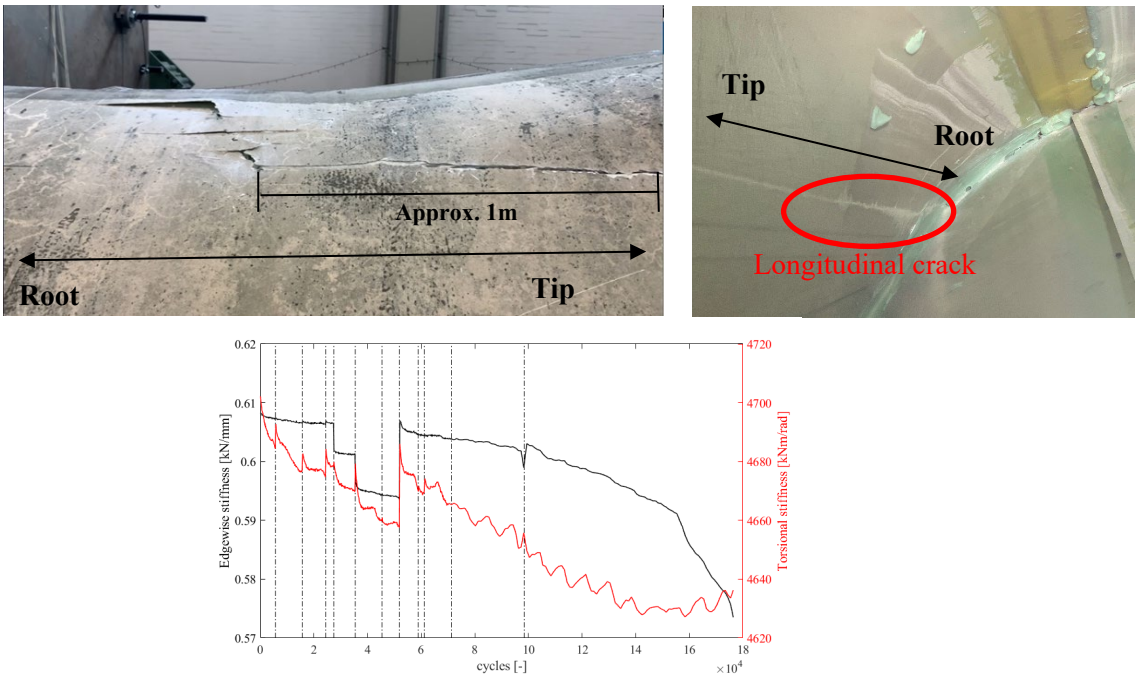

Figure 7. Picture presents the critical damage occurred on the 15m blade section of a 34m blade after 280.000 cycles in fatigue testing, where torsional loads are applied. The external condition of the blade (on the left), the crack observed internally (on the right). The length of the crack both internally and externally is around 1m. Plot presenting the change in edgewise and torsional stiffness (on the bottom).

Even though the measurements in the large-scale test focused on the bondlines of the retrofitted aft shear web, limited data is available for the position of the initial damage location (approximately 1-1.5m from the root towards the tip section). However, the initiated damage is highly relevant, as the results show that the application of torsional load components lead to critical damage in the root transition zone on the unsupported panels.

The potentiometer installed 200mm from the front of the aft shear web towards the root (approximately 3.8m from the root has captured out-of-plane deformations in the transition zone. Since the damage occurred further towards the root, the panel deformation is likely significantly higher where the panels are unsupported. At the position where the measurements were made, the aft shear web supported the blade shells which indicates that the out-of-plane deformation of the panels are likely lower in this area. The mounted wire potentiometer is presented in Figure 8 below.

Figure 8. The mounted wire potentiometer measured out-of-plane deformation of the blade panels. The potentiometer was installed 3.8m from the root and 200mm from the retrofitted aft shear web.

The findings suggest that in case the aft shear web is helping to reduce out-of-plane deformation where it is installed, increased "breathing" will occur on the blade further towards the root section which leads to skin delamination and that result in a catastrophic failure mode.

Additionally, a second 15m blade section of a SSP34m blade was tested with a 5cm crack introduced manually into the bondlines on both sides of the retrofitted aft shear web. The test was executed under the same conditions as the first fatigue test (100kN edgewise load component (F_Y) and 100kNm torsional moment (M_Z) with the frequency of 0.1Hz). However, the test was halted after approximately 12000 cycles due to technical issues with the mounting box girder installed onto the tip section of the blade which mounts the blade onto the test rig. During the 12000 cycles significant increase in out-of-plane deformation was observed, from the initial 10mm deformation, it increased to 13mm. as represented on Figure 9, below.

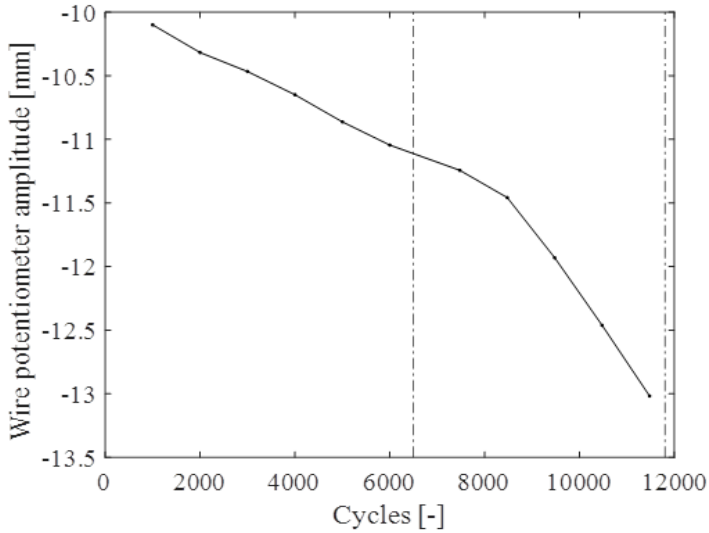

Figure 9. The measurements obtained from the wire potentiometer regarding out-of-plane deformation during the second test.

In Figure 9, a plot is presented of the magnitude of out-of-plane deformations and the nr. of cycles. A sudden drop (a drop in the plot shows an increase in the out-of-plane deformations) is observed on the plot at around 8000 cycles, show that damage is growing faster, hence is unstable. Upon inspecting the aft shear webs bondline, a clear crack propagation of over 10mm was observed on both bondlines of the aft shear web, see Figure 10.

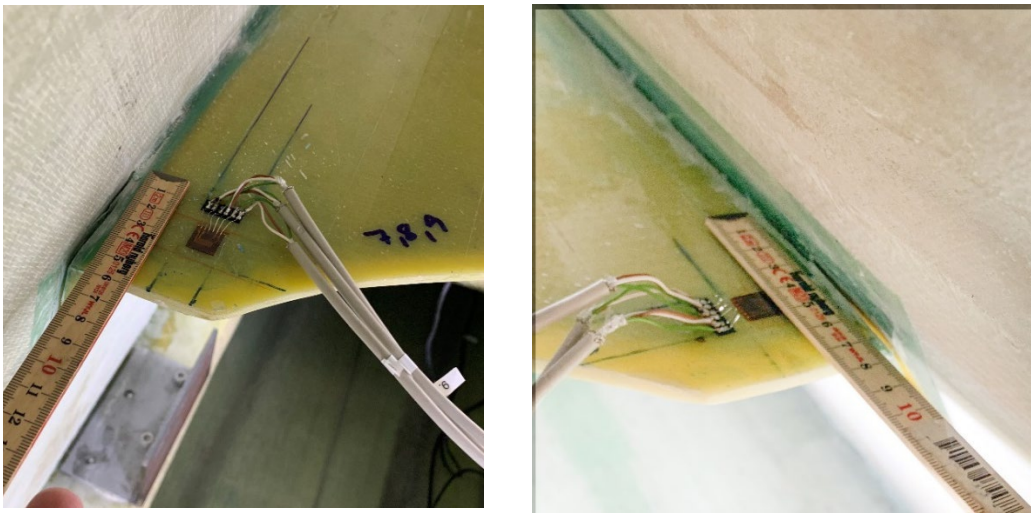

Figure 10. Approximately 10mm crack propagation on the Suction Side (on the left). Approximately 20mm crack propagation on the Pressure Side (on the right).

Figure 10 shows the results of inspection. A 10mm crack and a 20mm crack was observed on the SS and PS, respectively causing a halt to the testing.

In summary, increased "breathing" was observed when torsional load components were applied to the 15m blade cut-outs, leading to a severe damage during large-scale testing. This outcome was encountered during two separate experimental analyses, each revealing the extent of the damage caused by these loads. These tests led to the finding: the impact of torsional loads is not confined to only longer blades but also substantially affects shorter ones. Even a blade with a relatively short length of 34m

demonstrated vulnerability to torsional loads. This conclusion emphasizes the importance of considering torsional loads in the design and testing phases of wind turbine blades, regardless of their size.

4. FEM Analysis

Three different analyses have been conducted. Firstly, simulations were performed comparing the additional tip deflection and consequent torsional loads representing actual operational conditions to a scenario with only edgewise loads. This scenario is expressed in several tables below as "Only edge TTL", meaning that the loads are exclusively considered in the edgewise direction, from trailing edge to leading edge. Secondly, torsional moments have been quantified for different blade sizes, obtaining scaling factors for RTM and edgewise and flapwise RBM. Thirdly, 3D FEM analysis have been applied to determine the influence of torsional loads on peeling stresses and bending strains on three hotspots (damage prone regions) of the blade:

1. Max chord area, unsupported panels
2. Transition zone, fishmouth of the aft shear web
3. Transition zone, unsupported panels

Two failure modes are covered for these hotspots: shear web disbonding, and skin debonding.

These hotspots were selected based on the author's in-field experience regarding damage occurrence during operation.

Each hotspot is analysed for the blade position where the highest values were found. Two operational load positions, 90-degree azimuthal position and 270-degree azimuthal position have been used. To clarify this, the azimuthal degree indicates the position of the blade during rotation. As an example, 0-degree represents a blade in a vertical position with the tip pointing up, and 180-degree azimuthal position the blade is also vertical with the tip facing down. For further details, see Figure 11.

The two blade FEM models have been established using state-of-the-art structural and FEM numerical knowledge.

4.1. FEM Technical details

The FEM blades are modelled using 3D layered solids with eight nodes, each possessing composite properties, such as glass epoxy and pultruded carbon profiles in the spar cap, balsa wood in the inner third, and PVC foam in the outer region. These materials, with their biax, triax and unidirectional layers are built up in specified directions and enclosed by a core in the panels.

Regarding the FE model boundary conditions, all nodes are fixed in the root for translations. An MPC-element is used to offset reaction forces/moment at the Origo. The model uses large displacements with a load prescribed following a non-linear geometry analysis. This includes 10 load steps with equal load distribution and a follow-forces option is also used Convergence studies have been performed to ensure the results are reliable, as they guarantee the elements are adequately small.

This modelling approach is very effective at capturing out-of-plane deformations as well as strains and stresses in the lamina. This feature is used to extract strains from the outer and inner layer of panels and calculate bending strains.

The applied loads are calculated by adapting operational loads for specific blades familiar to the author and adjusting them to fit the 80m blade and the 120m blade. In the process, Bladena has gathered different load distributions from various manufacturers for different blade sizes over several years. In addition to this, Bladena has also received information on different Root Bending Moments (RBM) in both edgewise and flapwise direction. Bladena used a preprocessor from MSC-Software (Patran) to calculate the Root Torsional Moment (RTM). First the RBMs are verified to align with calculation from the manufacturer, and subsequently the RTM is extracted from Patran. An analytical calculation of the RTM, obtained by multiplying the edge- and flapwise loads by the "torsional arm" (deformation) across 12 sections along the blade, has been performed. The RTMs from numerical FEM and analytical calculations have been compared and very similar results have been obtained. It is important to note that

the flapwise loads are applied at the aerodynamic centre and not at the shear center, as an important contributing to the torsional loads would otherwise be neglected.

4.2. Operational loads cause extra Tip Deflection leading to additional Torsional Loads

The current design basis considers the loads associated with displacements in the edgewise and flapwise independently and not their combined three-dimensional effect equivalent to what is found under actual operating conditions.

This simplification implies a significant underestimation of the actual movements of the blades and thus of the forces/stresses that the blades are exposed to in real life. For the 120m blade the global edge tip deflections are presented in Table 2.

120m wind turbine blade	**Edge tip deflection [m]**
Only edge TTL	6.6
Operational loads, 90-degree azimuthal position	9.2

Table 2. Edgewise deflection for both operational loads, and only edge load component. 120m wind turbine blade.

Regarding the edgewise direction, blades are significantly stiffer than in the flapwise direction, but the deflection values increase from 6.6m to 9.2m when actual operating conditions are added. The increased edgewise deflections are equivalent to a loss of stiffness compared to the design basis. This effect will not only influence the tip deflection, but also the stresses in the max chord area and in the transition zone.

4.3. Quantification of Torsional moments

As also mentioned in the introduction section, the load contributions that introduce a root torsional moment on the blade arise from the aerodynamic forces and gravity working on the already deformed blade under operation. The aerodynamic forces can be divided in a purely flapwise component as well as a tangential component in relation to the rotor plane, acting as an edgewise load, in relation to the aerodynamic profile of the blade. Additionally, gravitational loads are also acting in the edgewise direction, see Figure 11.

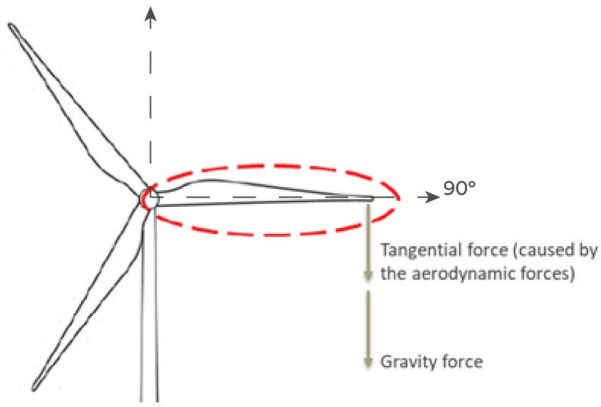

Figure 11. Investigated blade in 90-degree azimuthal position as the blade rotates. The arrows next to the forces indicate direction only, the gravity forces act at the center of gravity of the blade whereas the tangential forces (caused by the aerodynamic forces) act along the blade.

When the blade is loaded and deflected, torsional loads are generated. The edgewise aerodynamic loads working on a flapwise deformed blade twist the blade in a clockwise direction if the blade is seen from the tip towards the root. At the same time aerodynamic flapwise loads work on the edgewise deflected blade and the twist direction generated by this depends on the direction of the edgewise deflection. While the tangential aerodynamic loads (if the aerodynamic loads are split into two, based on directions, we can define normal direction and tangential direction) are always working towards LE, the gravitational load switch direction relative to the blade between the two horizontal positions. Figure 9 shows 90-degree azimuthal position where the aerodynamic tangential forces and gravity works in the same direction. For this position the flapwise loads generate a counterclockwise twist to the blade when seen from tip towards the root. Figure 10 illustrates the resulting torsional moments due to the operational loads.

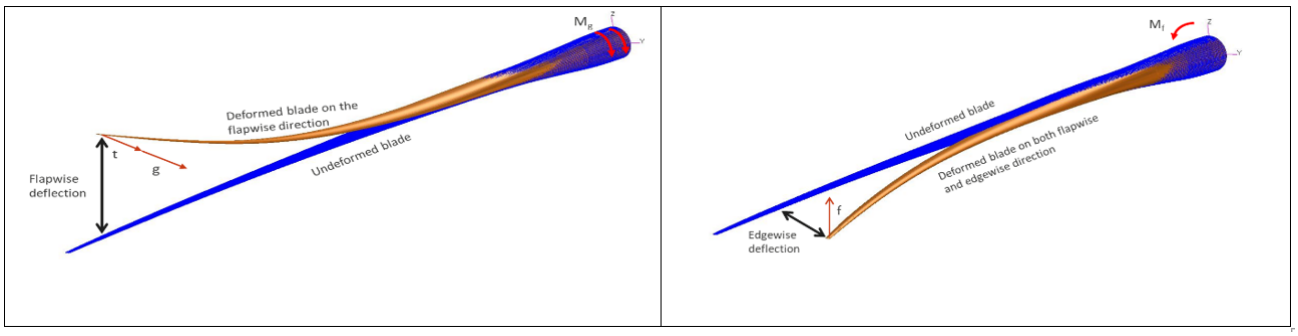

Figure 12. Left: RTM when gravity and tangential forces are in the same direction. Right: Root Torsional Moment induced by flapwise forces. Moment is acting in a different direction than the ones from the edgewise loads. On the figures "t" indicates tangential force and "M" indicates torsional moment.

A scaling study was carried out using two generic blade FEM-models, i.e., a typical 80m blade (corresponding to 7-9MW) and a typical 120m blade (corresponding to 15-18MW).

In the scaling study of the two blades, an 80m blade and a 120m blade, the blade characteristics can be compared. Both blades which are considered large (60m+), share a flatback design with two main shear webs and an aft shear web starting in the transition zone. They also both have carbon in the caps. Despite its large size, the 120m blade is very slender and lacks a clearly defined max chord, instead featuring a max chord region. This means that even though one blade is much larger, they have the same "max chord" profile length of approximately 5m. The sandwich panels are built up with layers of glass fibers (biax, triax, unidirectional).

The three torsional moment contributions and the total moment are listed in Table 3. It is seen that the total root torsional moment is 4 times higher in the 120m blade compared to the 80 m blade.

Torsional load contribution	Generic 80m blade	Generic 120m blade
Gravitational contribution	200 kNm	1600 kNm
Tangential contribution	160 kNm	700 kNm
Flapwise contribution	-160 kNm	-1500 kNm
Total	200 kNm	800 kNm

Table 3. The torsional moment contributions for 80m and 120m blades for 90-degree azimuthal position. A positive moment is defined as the moment that twists the blade clockwise if the blade is seen from the tip towards the root.

Table 4 below shows the result of a study conducted to understand how the RBM and RTM change for different blade sizes. The exponents shown below correspond to a curve fitting performed with the values from this study in which in the x-axis the blade length was presented, and the RBM or RTM in the y-axis. So RBM and RTM are represented as a power function with an exponent x.

$$f(x) = ab^x$$

Where:

- $f(x)$: RTM or RBM
- a: value different to 0
- b: blade length
- x: exponent shown in table below

Load direction	Exponent
Flapwise RBM	2.8
Edgewise RBM	3.4
Torsional RTM	4.0

Table 4. Exponent increase for as a function of blade length for flapwise RBM, edgewise RBM and torsional RTM.

In all cases, magnitudes increase as a function of the blade length, especially in the case of torsional RTM. The mathematical relationship between the three studied variables (Flapwise RBM, edgewise

RBM, and torsional RTM) and its dependency on blade length (exponent shown in Table 4) shows a scaling with a power law with a power of 4 for the torsional RTM.

Finally, Table 5 presents a list of potential failure modes and the impact on them from of torsional loads. Failure modes which are dependent on panel deformation e.g., breathing and CSSD are heavily impacted by the inclusion of torsional loads, whereas damages in the root (T-bolts, root inserts) are not impacted.

Failure mode	IEC 61400-5:2020	IEC 61400-23:2014	DNV-ST-0376:2021	Used in industry	Uncertainty of tools	Impact of torsional loads
Bondlines (Peeling test)	(2)	(1)	(3)	(YES)	MEDIUM	HIGH
Skin debonding from core (Test)	(2)	(1)	(3)	(NO)	MEDIUM	HIGH
Interlaminar failure (Bending test)	(2)	(1)	(2)	(NO)	LOW	HIGH
Global strain (Failure criteria)	(5)	(5)	(5)	YES	LOW	LOW
Shear web disbonding	(2)	(1)	(3)	(YES)	MEDIUM	HIGH
Root failures	(5)	(5)	(5)	YES	LOW	NO

Table 5. Table regarding potential failure modes and the impact of torsional loads on them, ref. [16] p. 46 (1 means there is no reference in the standard, 2 means it is mentioned briefly, 3 means that it is mentioned as "can be considered", and 5 means it is required in standards). The table does not take vibration issues into account. An additional column with the impact of torsional loads has been included. Regarding this column, it must be said that the impact depends on the section of the blade where this is analysed.

4.3 Impact of Torsional Loads on Selected Failure Modes

This sub-section addresses the impact of applying torsional loads in non-linear geometric 3D-solid FEM models for different failure modes.

The objective is to quantify the influence of torsional loads on variables such as peeling stresses, and bending strains, which have a direct relationship with some of the most common structural field damages seen during operational conditions.

The root transition zone of the blade has a complex geometry and contains tapering shell panels in 2 directions double curved in addition to the concave-convex double curved geometry. In addition, depending on the blade model, these panels in the TE box often have a large unsupported panel area in some sections of the blade, since the aft shear web usually starts around the max chord area or at the very end of the root transition zone.

4.4.1. *Shear web disbonding*

As explained in the introduction, shear web disbonding is a frequently occurring failure mode seen for a variety of larger blades. This failure mode is characterised by disbonds in the aft shear web bondlines, initiating from the spar cap fishmouth region. Thus, special attention has been aimed at blades which

have an aft shear web with a fishmouth shape, as well as traces of delamination in the area of the fishmouth foot, see Figure 2.

Consequently, peeling stresses is the main parameter to focus on in the 3D-solid FEM analysis in order to understand the possible initiation of this failure mode.

In the following, results from two different studies will be presented on this topic for two different blade sizes, namely 80m and 120m. The fishmouth region of the aft shear web is located between the trailing edge and the trailing edge shear web and situated at a distance of 3.5m towards the root for the 80m and 9,8m for the 120m blade. These are the positions where the aft shear web starts for the two blades with different length.

1. 80m wind turbine blade

Operational loads have been compared against only edgewise loads.

Results are presented in terms of maximum values. Maximum values show the highest stress or strain calculated by FEM in the selected hotspots. They are considered as being the most likely locations for initiation of damages. An increase of 40% in maximum peeling stresses can be observed in the transition zone due to the impact of torsional loads, presented on Table 6.

It cannot be stated whether this increase in stresses is critical or not, and no literature has been found for reference. Such an evaluation will vary from blade design to blade design. In addition, standard methodologies representing fatigue analysis such as SN curves are not considered to be accurate enough for the analysis of interlaminar strength (ref [21] and [22]). A correlation with field damage would be required in order to estimate peeling stress values that may lead to the initiation of the damage, particularly in the form of shear web disbonding.

However, it must be considered at this point that the transition zone is the main load carrying area of the blade. Thus, damages in this area can influence the structural integrity of the entire blade. Bondlines in this area may suffer from high peeling stresses caused by localised deformations, probably due to the breathing of the panels and the cross-sectional shear distortion of the structure, composed by the spar caps and the shear webs. Increases, like the 40% shown in this paper, may be enough to exceed the stress limit that can be carried by the bondlines.

Figure 13 below shows an example of where the peeling stresses are extracted from the 3D-solid FEM analysis.

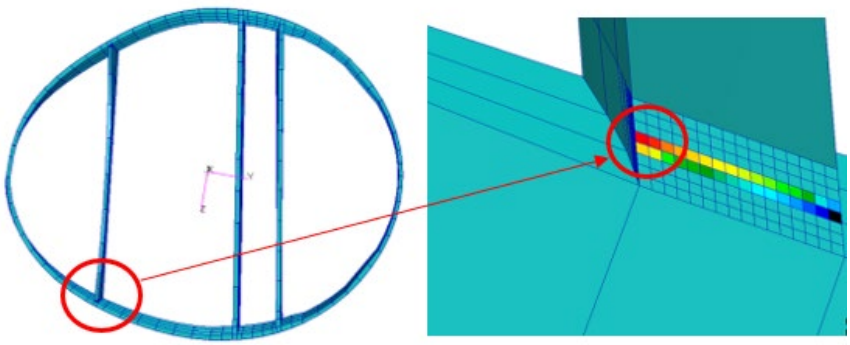

Figure 13. An example of the location where peeling stresses are extracted. The cross section is of a root-transition zone area and the peeling stresses are extracted at the aft shear web fish mouth foot as highlighted in red circle. The illustration is an indication of the increased peeling stresses in the investigated area.

2. 120m wind turbine blade

Again, a comparison between operational loads and edge loads as they are assessed in the current industry design basis has been established. As shown in Table 6, an increase of 23% is deducted from the application of torsional loads.

When comparing results from both the 80m blade and the 120m, see Table 8, it can be observed that, on one side, the values for the 120m blade are between 14% and 30% higher than for the 80m. This result is expected from a theoretical point of view, as the larger torsional arm created in the case of 120m blade, should generate a higher RTM and consequently higher peeling stresses in sensitive structural areas. It may be noted, that for the generation of torque, there must be a force component applied in the perpendicular direction to the line of action of this force from the point around which it is calculated. In other words, if the torsional arm increases, the twisting of the structure will be higher, which will lead to deformation of the blade cross section. As a result, increase in peeling stresses due to both cross section shear distortion and local bending of the unsupported panels between the trailing edge and the aft shear web in the transition zone will be present.

On the other hand, by analysing the percentage increase due to torsion, it can be seen how the impact of torsional loads is increasing faster in the 80m blade than in the 120m blade. The reason for the smaller increase is most likely due to the position of the aft shear web, which is very sensitive.

The most important observation is that for all blade types there is a significant increase in the peeling stresses when torsional loads are applied.

Blade	**Peeling stresses. Operational 90-degree azimuthal position [Mpa]**	**Peeling stresses acc. To current standards [Mpa]**	**Increase due to torsional loads**
80m	1.4	1	+40%
120m	1.6	1.3	+23%
Comparison	+14%	+30%	

Table 6. Comparative table for shear web disbonding. Max values

When comparing the max values for operational load 90-degree azimuthal position between the 80m blade and the 120m, an increase of 14% is found. For the case of pure edgewise load case, the value reaches a +30%. In this case, results are aligned with expectations, showing that peeling stresses increase with the blade size.

Consequently, the reason for the high number of failures due to shear web disbonding in the transition zone is probably due to torsional loads in large wind turbine blades. Only with field data will it be possible to fully validate the results herein. For this purpose, a validation process would be required, in which field and test measurement campaigns would be carried out in specific critical hotspots, measuring the physical response of the blade, and obtaining essential knowledge to validate the FEM models and numerical results obtained. A validation process is considered a key element to reduce risk in large blades. For further information, see ref. [10].

4.4.2. *Skin (face sheet) Debonding from Sandwich Core in the Root Transition Zone*

This failure mode is also more commonly seen in large blades in operation based on the author's in-field experience. Breathing of the panels due to out-of-plane deformations will potentially initiate skin debonding between the thin skins and the balsa or foam core of the sandwich shell panels. When

sandwich panels are subjected to bending there is a risk that the interlaminar strength is not sufficient, causing skin debonding to initiate. If this occurs the bending stiffness of the sandwich panel will decrease significantly, and further crack propagation might develop rapidly. As a result of this, measuring bending strains through FEM will provide an indication of the behavior and possible breathing and bending of the panels which is understood as a possible root cause of this failure mode. Bending strains are calculated as the absolute difference between the outer strain and the inner strain of the panel.

The performed FEM analysis allows for comparison of the bending strains due to only edgewise loads with the operational loads. Results are presented for both the 80m and for the 120m wind turbine blades. For the 80m blade, the bending strains have been measured at 3m from the root and 0.7m from the TE. For the 120m blade, the measured area is around 8m from the root and 1.2m from the TE in the chordwise direction.

The strain value is taken in the surface plane direction transverse of the blade profile (as opposed to longitudinal strains). This direction is best at capturing out-of-plane panel deformation. The complex geometry of the area changing from concave to convex and tapering in two directions is the main explanation for that the out-of-plane deformations are highest in this region, see figure 3.

Results for bending strains will in some cases give negative values, while in others they will be positive. A negative strain is defined as whenever the bending is experienced inwards in relation to the blade cross section, and a positive value indicates that the bending is outwards. Whether positive or negative is not important; the importance is the magnitude, as the focus is on the amount of bending, regardless of whether the bending is inwards or outwards.

1. 80m wind turbine blade

Transition zone. Max values. Results are shown in Table 7..

Bending strains increase due to the increased level of bending and breathing of the panels. The transition zone is the main area of the blade carrying the loads, meaning that even small modifications in the load distribution may have an impact in this structurally critical area.

It can be seen how bending strains are increased 550% under the impact of torsional load. It can also be observed that the direction of strains changes from positive to negative. This sign is not important for the interlaminar stresses between the layers.

One reason that could explain this finding could be that when operational loads are included in the analysis, the panels may suffer an increased bending due to the loss of stiffness in the edgewise direction, as seen in Table 2. Here the tip deflection was compared with and without applied torsional loads for the 120m blade, concluding that operational conditions lead to an extra deflection due to the combined loading scenario. This loss of stiffness experienced for the 120m, is expected to also happen for the 80m blade, as this blade will also suffer from a softer edgewise deflection that could explain the big percentual difference in the impact of torsional loads.

Max chord area. Max values. Results are shown in Table 7.

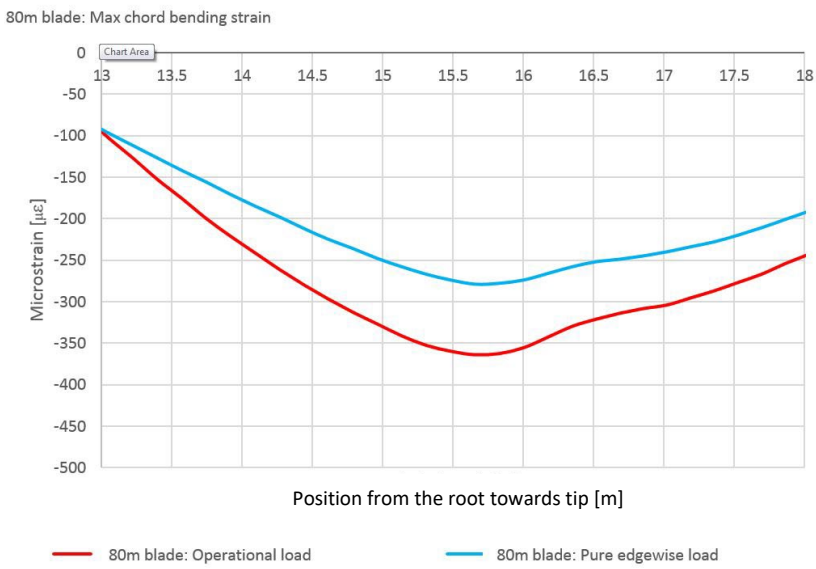

Figure 14. Bending strain comparison for the 80m blade in the max chord area. Operational loads 90-degree azimuthal position vs Only Edgewise loads.

For the max chord area Table 10 shows that bending strains increase around 30% whenever torsional loads are included.

It is also important to highlight that values for operational conditions are lower in the max chord area (360με) than in the transition zone (450με) which strengthens the hypothesis that the transition zone is the most critical and sensitive area from a structural point of view.

2. 120m wind turbine blade

Transition zone. Max values:

The evaluation focuses on the transition zone region, specifically between 8m and 9m along the blade length. The increase in the bending strains due to torsional loads are 120%, as can be seen in Table 7.

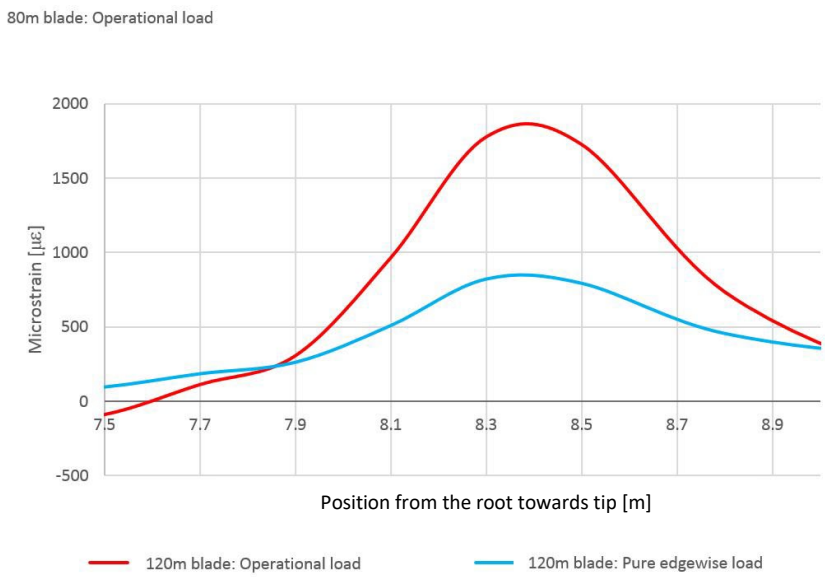

Figure 15. Bending strain comparison for 120m blade in the transition zone PS, operational load 270-degree azimuthal position max values vs Pure edgewise load max values.

Table 11 also indicates that bending of the panels is more severe in a 120m than in the 80m blade, shown in table 9. The difference in bending strains with operational loads reaches a +40% (630με vs 450με).

Consequently, it may be concluded that bending strains in the transition zone could increase linearly to the size of the blade.

Max chord area. Max values, results can be seen in Table 7.

Regarding the max chord area, the increase in the bending strain due to torsional loads is of around +47%.
Summary table for skin debonding with max values is shown in Table 7.

Summary. Bending strains	**Operational [με]**	**Bending strains acc. To current standards [με]**	**Increase due to torsional loads**
80m TZ	-450	69	+550%
80m Max chord	-360	-280	+29%
120m TZ	630	430	+46%
120m Max chord	-1090	-740	+47%

Table 7. Comparative table for skin debonding with max values.

Two main observations and results from the analyses can be highlighted:

- 80m blade vs 120m blade: the bending strains of the larger blade are significantly higher than for the smaller one, which emphasizes the thought that large blades have a much smaller structural reliability than medium or small blades. When values are compared between the 80m blade and the 120m applying operational loads:
    - Max chord area, transverse bending strains: +200% (from -360με to -1090με)
    - Transition zone panels, transverse bending strain: +40% (from -450με to 630με)

- Transition zone vs Max chord area: the transition zone does not always experience higher bending strains than the max chord area.
    - 80m, transverse direction bending strains: +25% (from -360με to -450με)
    - 120m, transverse direction bending strains: -71% (from -1090με to 630με)

5. Impact of torsional loads on lifetime – Discussion of results

The information presented in this paper emphasizes the importance of the torsional load components in order to correctly assess the durability of a given blade. Publicly available information on field damages, experimental analysis, and numerical models all points in the same direction: the larger turbine blades necessitate high maintenance costs (ref.[20.]).

As a result, it seems logical that the wind industry would adapt to the ongoing changes and challenges. This would mean reassessment of the design principles and O&M (Operation and Maintenance) strategies of large modern blades. Moreover, predicting the lifetime of these blades is a complex task, particularly because the traditional S-N curve method may not be accurate enough when it comes to analysing interlaminar strength (ref [21] and [22]). It is a well-established understanding among composite material experts that the S-N curve approach cannot be used to predict the lifetime of bondlines within these materials. Instead, these experts, including the authors of this paper, propose using a fracture mechanics approach. This method offers increased accuracy and allows for the implementation of a damage tolerance approach. The damage tolerance approach is about predicting when damage will occur and understanding how the structure will behave once a damage is present. Our main research project, see ref. [10], over the past two years, has been focused on these aspects.

The experimental analysis resulted in two different failure modes, both of which are considered critical. Meaning that, if damage types like the ones observed (such as delamination, aft shear web disbonding) occur in field, the turbine must be immediately stopped to avoid blade collapse. During testing, the applied loads were approximately 50% higher than what a blade on a 1.5MW turbine would experience; therefore, damage initiation was expected, though there was uncertainty about the specific failure mode. The observed failure modes confirmed that bending of the unsupported panels under applied torsional load components can lead to significant problems. In the case of the first blade, the clear decrease of global stiffness indicated the damage (a delamination leading to longitudinal crack, approximately 1m in length) whereas in the case of the second blade, a sudden increase in out-of-plane deformation indicated the shear web bondline disbond. As previously mentioned, the occurrence of such damages in field could be minimized by following the right strategy.

The majority of our research projects' participants and partners are Wind Turbine Owners whose goals are to minimize operating expenses (OPEX) and maximize the annual energy production (AEP). They are not typically involved in the design process, and therefore have not adopted the classical damage tolerance approach. However, in our views, the traditional methods are viewed from a perspective that is relevant not only to wind turbine owners but, hopefully, to manufacturers and companies involved in service and management. Doing this aims to bring a fresh understanding and approach that benefits all parties involved.

6. Conclusions

The current design and validation testing of large wind turbine blades omit substantial loads on the blades and that these omissions may very well explain the high level of unwanted maintenance costs that are currently found in the industry on large blades; an effect which increases with increasing blade lengths. In comparison with an 80m long blade, the bending strains in a 120m long blade were 200% higher in the max chord region and 40% higher in the transition zone (max chord: from -360με to -1090με; transition zone: from -450με to 630με).

The paper presents non-linear 3D-solid FEM comparisons between different load scenarios as they come out of the current design practice and stresses as they come out when the more realistic 3D non-linear behaviour of the blades is accounted for.

Numerical analysis using non-linear geometric 3D-solid FEM, for the study of shear web disbonding and skin debonding, can conclude that peeling stresses and bending strains are found significant for large blades due to the high torsional loads generated when the blade is in operation.

The results may be summarized as follows:

- The torsional loads that are found under actual operating conditions cause additional and critical out-of-plane deformation of the unsupported panels and also distortion effects such as CSSD and breathing. The localized deformations cause peeling in the bondlines, interlaminar stresses between the composite layers, and in between the sandwich skin and the core material. Layered composite structures and adhesive bondlines do not have a high load carrying capacity for those failure modes.
- The edgewise tip deflection increases by 40% for a 120m blade when the non-linear 3D behavior is accounted for. Amongst others, the larger deflection implies a loss of stiffness which in turn leads to significant increase in bending stresses and peeling stresses.
- Scaling factors have been quantified concluding that RTM's increase with a power of 4 with blade length.
- Experimental testing using large-scale section testing has demonstrated that critical damage in the root transition zone appears when torsional fatigue loads are applied.
- On the second blade shear web disbanding occur and showed an unstable crack development

It should be noted that even though the authors are confident that the results from the FEM models used for the study are valid, it should also be considered that the operational loads used for the analysis may differ from reality, as field measurements for large blades were not available thereby it is not sufficiently covered in this study. Also, layup and geometry are not accurate from any specific blades in the field and therefore, results must be perceived as a trend rather than accurate values.

However, despite any uncertainty of the results, the value of the FEM analysis results, and their conclusions are considered to be significant because the results demonstrate that critical loads are not accounted for in the current industry practice.

7. Recommendations

Taking all this into consideration, some areas have been identified which could potentially help to mitigate the risk of suffering damages from some of the structural damages related to torsional loads. The following recommendations are areas recommended to the wind energy industry to consider. We believe that a joint-venture project concerning the topic would be beneficial for the whole industry.

<u>Suggestion 1. Application of torsional loads during the static blade full scale testing program</u>

The full-scale testing program following IEC-61400-23 standard requires both flapwise and edgewise loads but in separated load cases (ref.[19.]). The static pull is close to the shear centre, hence almost no torsional loads are applied. The importance of both torsional loads, and a combined load case is recognised, but no obligation is imposed.

As an example, the IEC-61400-23 states that "the flap and lead-lag sequence of testing may be performed on two separate blades. However, if an area of the blade is critical due to the combination of flap and lead-lag, then the entire test sequence shall be performed on one blade" (ref.[19.]). The consideration of whether an area of the blade is critical or not due to the combination of loads is open to interpretation, meaning that freedom is given to applying or not a combined loading full scale test.

Another example that emphasizes that torsion is understood as a relevant matter, but not forced to be considered, is the following quote from Annex E in the same IEC-61400-23: "if torsion loads are significant in the structural design of the blade they should be included in the test" (ref.[19.]). Again here, it is subjective the establishment of whether torsion loads are critical or not. And even if they are considered as significant, the word "should" indicate a recommendation, not an obligation.

Therefore, the application of the torsional load components is suggested, as more realistic scenario, but nothing is imposed. As stated also in DNV's whitepaper, see in ref. [2], with the increasing size, the torsional loads and displacement of the shear centre are significant contributors to loading.

If the combination of loads were applied, with an offset, shown on the sketch in Fig. 18, the local deformations and distortion effects (CSSD and breathing) will be representative. To incorporate the combined flap- and edgewise loads, the blade was tilted 30 degrees in the direction of the leading edge toward trailing edge during the full-scale test performed in an earlier executed full-scale blade test study, see ref. [1]. At this full-scale test, the purpose was also to test the buckling capacity of the trailing edge. In this paper the focus is on the structural strength of the max chord region and the root transition zone and therefore the sketch show another load direction, in the positions where the torsional loads are highest.

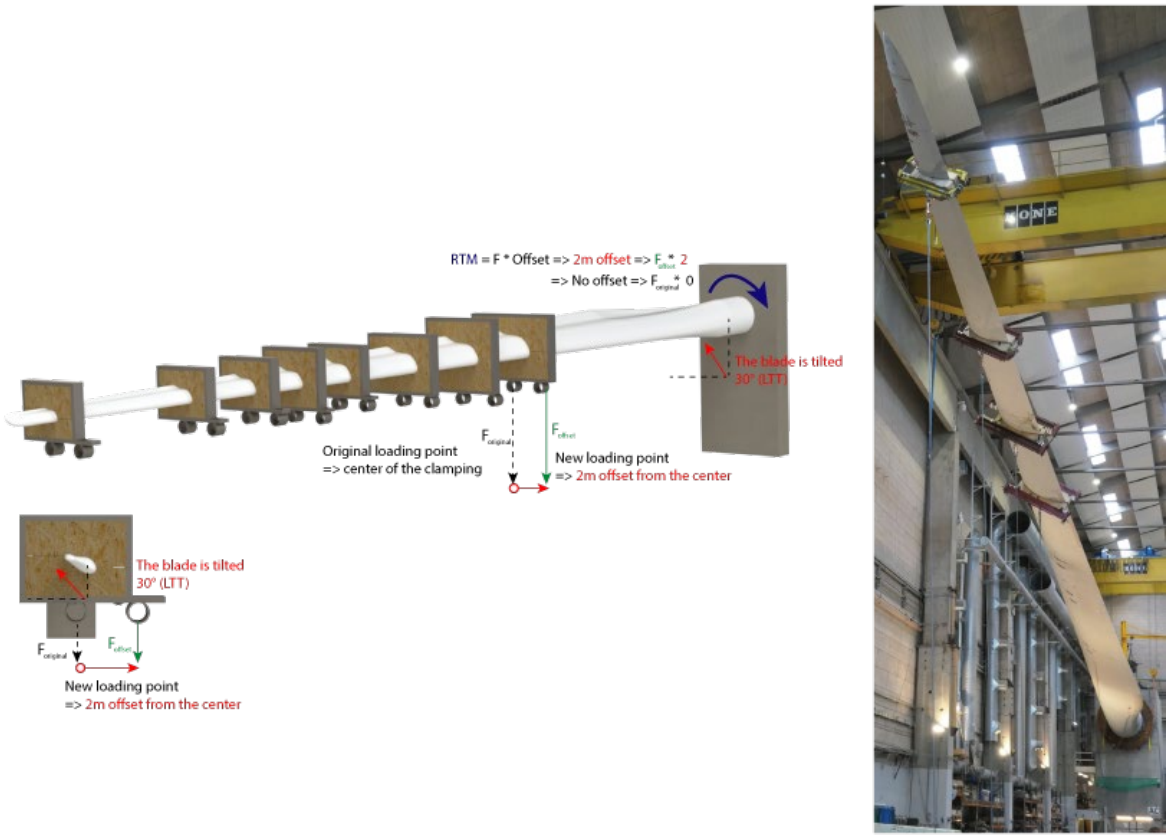

Figure 16: Sketch of a full-scale static test setup with applied torsional load components (left). Photo to the right show a full-scale test of a LM58,7m blade with combined statis loads performed at a commercial test center in collaboration with LM-Windpower and Bladena, see ref. [1] EUDP RATZ project.

This full-scale static test campaign is fast and easy to perform, and the costs are low. Furthermore, the additional load case can be done before the certification fatigue test program is started, and this is important since the measurement, is needed as early, as possible in order to validate FEM-models. When the FEM model is validated the boundaries for of the performed fatigue test sub-component program, can be updated.

More details regarding the needed measurement and the validation program can be found in the following two suggestions. Fig. 18 includes a photo from a full-scale test, Bladena and LM WindPower performed together in a commercial test centre. The static full-scale test with combined load was successfully performed, but at that time the test was performed, the knowledge about size of the torsional loads was known and furthermore the blade was only 58,7m, so the torsional arm offset should not have been as large as illustrated on the sketch.

The calculated torsional arm offset for a 120m blade has been calculated to be approximate 2m offset from the shear centre. 8 load clamps have been estimated, but of course this has been analysed for the actual blade and it can also be considered not to have the same offset for all load clamps, as long the sufficient torsional loads are applied it is not so important how it done.

Suggestion 2. Additional measurements

During a full-scale test campaign, additional measurements, are recommended to be implemented to identify localized deformation in the critical inner third of the blade e.g., cross-sectional shear distortion and breathing. This can be considered as a relevant step prevent from some of the failure modes here studied, as an example, the phenomenon "breathing" of sandwich panels in the trailing edge region, can influence both the formation of transverse cracks due to skin debonding followed by skin fatigue cracks, and the opening of the trailing edge due to high peeling stresses in the adhesive bondlines close to the trailing edge.

The additional measurements would also help to validate the FEM-simulations, so the boundaries for the fatigue sub-component test program for a lifetime estimation can be updated.

Moreover, back-to-back strain gauges on the unsupported panels in the transition zone is highly recommended. By measuring back-to-back strains, the localized bending causing potential critical interlaminar stresses can be determined.

Suggestion 3. Torsional loads during the 3D FEM modelling

Modern aero-elastic load simulations include the torsional loads in the analysis. However, according to the author's knowledge, these loads are not always included in the following non-linear 3D FEM analysis. This will also result in insufficient loading applied to the sub-component fatigue test program.

If the above three suggestions are implemented, potential issues can be found, and design improvements can be performed before the turbine is in operation.

8. Acknowledgement

Bladena would like to acknowledge the Energy Development and Demonstration Program (EUDP) for financial support under the grant number: 64021-1054 CORTIR II Project. Within the frame of the CORTIR II project considerable work has been done by DTU Construct regarding the experimental analysis and Global Wind Service supporting the large-scale test program and visualization work on several illustrations by Kirt X Thomsen.

References

[1] Bladena and Partners, (2019), "Project Report: Root Area Transition Zone RATZ and Reduction O&M cost of WT blades, Energy Development and Demonstration Program (EUDP) RATZ project, 64015-0062,", https://www.bladena.com/uploads/8/7/3/7/87379536/eudp_ratz_-_project_final_report_-_eudp_ref._j64015-0602.pdf

[2] Griffin, D.A., (2023), "The challenges of wind turbine blade durability" DNV Whitepaper, 2023, https://www.dnv.com/Publications/the-challenges-of-wind-turbine-blade-durability-243601

[3] Renews.biz, (2020), "Vestas, EDPR probe blade failure at Ohio wind farm.", Renews 2020 September 9. https://renews.biz/63000/vestas-blade-failure-at-edps-ohio-wind-farm/

[4] Harrison, C., (2019), "Limitations of legacy certification standards and benefits of new standards demonstrated on a100m wind turbine blade", DNVGL, WindEurope Offshore Conference, Copenhagen, 2019 November.

[5] Rajgor, G. (2022). "GE Renewable Energy investigates second Cypress wind turbine failure in two months", Windpower Monthly, 2022 March 16. https://www.windpowermonthly.com/article/1749796/ge-renewable-energy-investigates-second-cypress-wind-turbine-failure-two-months

[6] Bladena and Partners, (2021), “Cost and risk tool for interim and preventive repair (CORTIR) EUDP project 64018-0507 – Final Report”, https://www.bladena.com/uploads/8/7/3/7/87379536/eudp_cortir_-_project_final_report_-_ref._64018-0507.pdf

[7] Waldbjørn, J.P., Berggreen, C., Ahmed, S., Nagy, T., “Large-scale fatigue testing of a retrofitted 3rd shear web in a 34m wind turbine blade section” DTU Construct & Bladena, 2023

[8] Bladena, (2022), “Risk considerations on upscaling wind turbine blades”, Bladena whitepaper, 2022. https://www.bladena.com/uploads/8/7/3/7/87379536/white_paper_scaling_and_risk_bladena.pdf

[9] Bladena, (2022), “Structural weaknesses of blades in operation” Bladena whitepaper, 2022. https://www.bladena.com/uploads/8/7/3/7/87379536/whitepaper_1_structural_understanding_bladena_13.04.2022_compressed.pdf

[10] Bladena and Partners, (2023), “Cost and risk tool for interim and preventive repair (CORTIR Phase II) EUDP project 64018-0507 – Final Report”

[11] Karlsen, T. (2021), “76 meter langt turbine blad deiset i bakken – kan ikke si hvor utbredt turbinen er i Norge”, Teknisk Ukeblad, 2021 November 15. https://www.tu.no/artikler/136-meter-langt-turbinblad-deiset-i-bakken-kan-ikke-si-hvor-utbredt-turbinen-er-i-norge/515102

[12] Brøndsted, P., & Nijssen, R. (Eds.) (2023), “Advances in wind turbine blade design and materials.” Woodhead Publishing. Woodhead Publishing Series in Energy No. 47 http://www.woodheadpublishing.com/en/book.aspx?bookID=2548

[13] Jensen, F.M., "Ultimate strength of a large wind turbine blade," Risø DTU, PhD Thesis, 2008. https://backend.orbit.dtu.dk/ws/portalfiles/portal/5434131/ris-phd-34.pdf

[14] Bladena and Partners, (2016), “Torsional Stiffening of Wind Turbine Blades - Mitigating leading edge damages, EUDP project, 64013-0115”, https://www.bladena.com/uploads/8/7/3/7/87379536/eudp_lex_project_final_report_september_2016.pdf

[15] Waldbjørn J.P., Buliga A., Berggreen C., Jensen F.M., (2020), “Multi-axial large-scale testing of a 34m wind turbine blade section to evaluate out-of-plane deformations of double-curved trailing edge sandwich panels within the transition zone” DTU and Bladena journal paper, 2020, https://journals.sagepub.com/doi/abs/10.1177/0309524X20978408

[16] Bladena and partners, (2022), ”Wind turbine blades - Handbook”, Edition 2022 CORTIR, EUDP.

[17] Jensen F.M., Falzon B.G., Ankersen J., Stang H., (2005), “Structural testing and numerical simulation of a 34m composite wind turbine blade”, Composite Structures, October 2005, https://www.sciencedirect.com/science/article/abs/pii/S0263822306002480

[18] Gurit, (2020), “Ampreg 22 – Epoxy Laminating System”, https://pdf.directindustry.com/pdf/gurit/ampreg-22-epoxy-laminating-system-v17/37817-79061.html

[19] International Electrotechnical Commission, (2015), “International Standard: Wind turbines – Part 23: Full-scale structural testing of rotor blades”, IEC 61400-23 Edition 1.0

[20] Wood Mackenzie, (2019), “Unplanned wind turbine repairs to cost industry $8 billion+ in 2019”, Wood Mackenzie: One minute read press release https://www.woodmac.com/press-releases/unplanned-wind-turbine-repairs-to-cost-industry-$8-billion-in-2019/

[21] M. Quaresimin, M. Ricotta, (2005), “Fatigue behaviour and damage evolution of single lap bonded joints in composite material”, University of Padova, Italy, 2005

[22] A. J. Kinloch, (1997), “Adhesives in engineering”, University of London, 1997.